Intrinsic Relationship between Anatomy, Kinematics and Injuries of Knee Joint under Various Vehicle-to-Pedestrian Impact Orientations

Jisi Tang, Qing Zhou

I. INTRODUCTION

Considering the complicated anatomy and frequently reported injuries, the knee joint has received special attention in pedestrian safety protection. There have been extensive studies on biomechanics and injury mechanisms of the knee joint in vehicle-to-pedestrian accidents. Reference [1-2] demonstrated experiments examining kinematical response and ultimate strength of the joint structures under two impact severities. Kerrigan et al. acquired a more accurate measurement of joint stiffness and failure threshold by leveraging well-designed test apparatus and data processing approach [3]. Conventionally, knee joint kinematics was approximated as two-dimensional under lateral impact, and quantitatively characterised by lateral bending angle and shearing displacement. However, in real-world accidents, orientation of impact follows a distribution other than pure lateral configuration, and therefore, the kinematics of the knee joint cannot always be simplified as a planar type. Besides, anatomy of the knee joint is anisotropic in three-dimensional view. The implication is twofold: 1) the conventional two-dimensional characterisation has discrepancy to some extent, making it necessary to develop a three-dimensional version to consider the out-of-plane components; and 2) influence of the structural anisotropy on joint kinematics and injuries need to be investigated.

To address these issues, in this study, we first built a systematic framework to stepwise decompose the overall movement of a pedestrian knee joint into six degrees of freedom (DOF), then morphed the GHBMC simplified pedestrian model (M50-PS, version 1.1.4) into an obese individual using the parametric human body modelling method, and simulated a matrix of vehicle-to-pedestrian impact scenarios. Patterns of the kinematical responses and the correlation with tissue-level injuries were investigated. Influence of structural anisotropy on joint response was analysed, and its implication on countermeasure design was discussed.

II. METHODS

Framework of Decomposing Knee Joint Kinematics

In general, knee joint kinematics, also referred to as tibial movement with respect to the femur, is of six DOFs from a mechanical point of view – three translational and three rotational, respectively (Figure 1c, d). The first task of the current study was to develop a systematic framework to conduct component-wise decomposition of the overall movement and specify magnitude of motion associated with each DOF.

Two triplets of nodal coordinates were selected on the femur and tibia and to define their rigid-body motion. An origin was fixed at the intercondylar eminence of tibia. Resultant translation in knee joint kinematics is the trajectory of the origin between configurations and resultant rotation is overall movement deducting the translational part (Figure 1a). An orthogonal coordinate system was defined by referring to [4], which has three axes: 1) flexion axis $\boldsymbol{u}_F$ is the transepicondylar axis connecting medial and lateral epicondyles; 2) abduction (lateral bending) axis $\boldsymbol{u}_A$ is normal to the plane spanned by $\boldsymbol{u}_F$ and the longitudinal axis of tibia; and 3) internal rotation axis $\boldsymbol{u}_I$ is cross product of $\boldsymbol{u}_F$ and $\boldsymbol{u}_A$ (Figure 1b). Once defined, the coordinate system was attached to tibia to characterise the tibiofemoral movement. The resultant translation was decomposed by doing an inner product with basis vector associated with each translational DOF, regardless of the order (Figure 1c). Based on Euler's theory, any rotation in three-dimensional space comprises a group of three rotations about pre-defined axes (Figure 1d). Angles corresponding to the rotations are named Euler angles. In the current study, we developed an intuitive and practical approach with construction of rotation matrix and calculation of Euler angles being separated.

Q. Zhou (e-mail: zhouqing@tsinghua.edu.cn; tel: +86-10-6278-8689) is a Professor of Mechanical Engineering, J. Tang is a Research Engineer, both in the School of Vehicle and Mobility at Tsinghua University, Beijing, China.

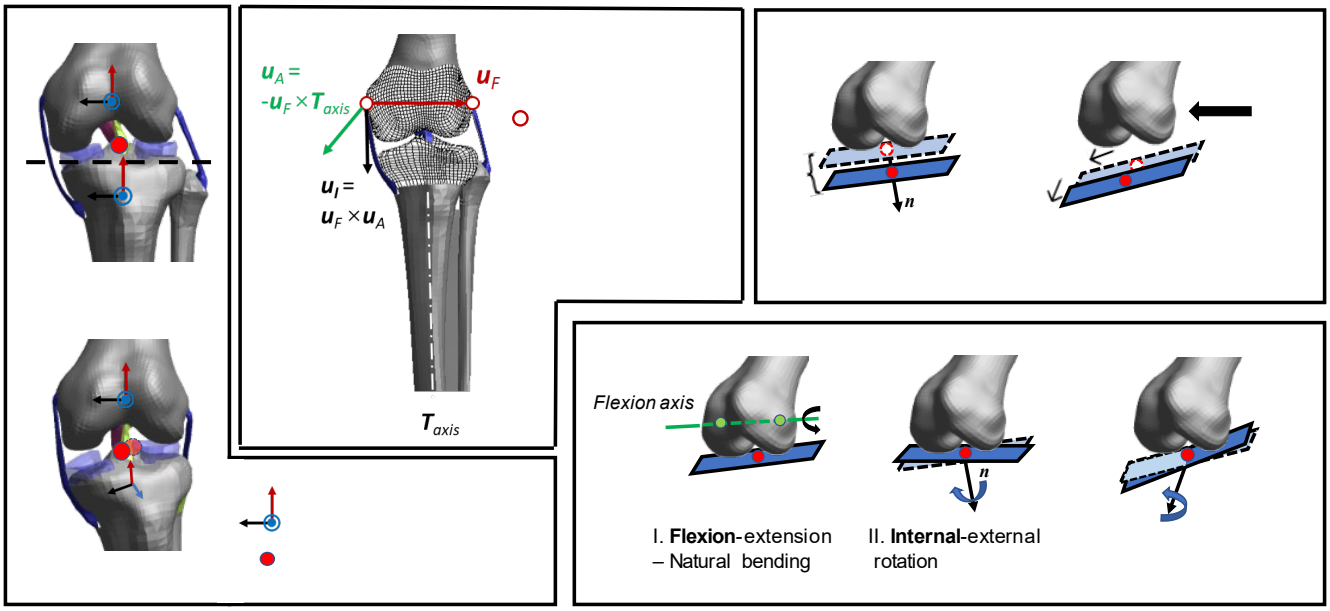

Figure 1. (a) schematic of knee joint kinematics; (b) definition of anatomical axes in motion decomposition; (c) component-wise decomposition of resultant translation and illustration of translational DOFs; (d) illustration of rotational DOFs and Euler's theory-based decomposition of resultant rotation. In (c) and (d), it is a left knee joint in antero-lateral view, with positive directions for each DOF marked with arrows and bolded annotation.

Given two orthonormal coordinate systems named $\boldsymbol{C_1} = [\boldsymbol{g_1}, \boldsymbol{g_2}, \boldsymbol{g_3}]$ and $\boldsymbol{C_2} = [\boldsymbol{g_1}^*, \boldsymbol{g_2}^*, \boldsymbol{g_3}^*]$ respectively, where $\boldsymbol{g_i}$ and $\boldsymbol{g_i}^*$ are corresponding pairs of basis vectors. Rotation matrix representing transformation from $\boldsymbol{C_1}$ to $\boldsymbol{C_2}$ and satisfying the relationship $\boldsymbol{C_2}=\boldsymbol{R}\cdot\boldsymbol{C_1}$ is defined as $\boldsymbol{R} = \boldsymbol{C_2}\cdot\boldsymbol{C_1}^T$.

Referring to Euler's theory, the overall rotation matrix $\boldsymbol{R}$ is multiplication of a group of rotation matrices. Mathematically, each sub-rotation is a transformation between coordinate systems. The transformation is represented by a tensor, which is the function of the rotation axis $\boldsymbol{u}$ and angle θ, explicitly written as (1),

$$\boldsymbol{R}(\boldsymbol{u},\theta) = cos\theta\cdot\boldsymbol{I} + sin\theta\cdot\boldsymbol{u}_x + (1-cos\theta)\cdot\boldsymbol{u}\otimes\boldsymbol{u} \tag{1}$$

where $\boldsymbol{I}$ is the identity matrix; $\boldsymbol{u}_x$ is skew-symmetric matrix spanned by $\boldsymbol{u}$; and $\boldsymbol{u}\otimes\boldsymbol{u}$ means tensor product between axis vectors. Corresponding matrix-representation of (1) could be found in [5]. With axes of rotations being defined (Figure 1b), the main goal of the decomposition is to compute the Euler angles θ_F, θ_I and θ_A at a given instant. Based on the preceding analysis, the overall rotation matrix $\boldsymbol{R} = \boldsymbol{C_2}\cdot\boldsymbol{C_1}^T$ has a form as (2),

$$\boldsymbol{R} = \boldsymbol{R}_A(\boldsymbol{R}_I\cdot\boldsymbol{R}_F\cdot\boldsymbol{u}_A,\theta_A)\cdot\boldsymbol{R}_I(\boldsymbol{R}_F\cdot\boldsymbol{u}_I,\theta_I)\cdot\boldsymbol{R}_F(\boldsymbol{u}_F,\theta_F) \tag{2}$$

where $\boldsymbol{R_F}$, $\boldsymbol{R_A}$ and $\boldsymbol{R_I}$ are sub-rotation matrices corresponding to flexion, adduction and internal rotation respectively. Calculation of the angles follows an intrinsic-rotation manner. Axis of the following step is updated by rotation in previous step (e.g. $\boldsymbol{R_I}$ constructed with rotated axis – $\boldsymbol{R}_F\cdot\boldsymbol{u}_I$ – instead of the original axis $\boldsymbol{u_I}$).

By transforming (3) into matrix-representation, the whole system has nine equations (note $\boldsymbol{R}$ is 3x3 in dimension) and three independent variables – θ_F, θ_I, θ_A. Considering $\boldsymbol{R}$ is an orthogonal matrix, its components satisfy orthogonality and normalisation condition – $\sum_{k=1}^{3} R_{ik}R_{jk} = 1$ when $i = j$, 0 when $i \neq j$. The conditions provide six extra constraint equations and make the problem solvable in MATLAB.

Simulation of Vehicle-to-pedestrian Impacts and Data Analysis

As a part of systematic study on effect of body size and posture, a morphed obese model (175 cm and BMI 40) in standing posture based on GHBMC simplified pedestrian model (M50-PS, version 1.1.4) was used to represent human body (Figure 2a). Details of the mesh morphing procedure are documented in [6]. Tissue failure via element deletion was toggled off to avoid uncertainties brought by failure threshold or mesh distortion, which would allow us focusing more on the anatomy and orientation effect. The simulation matrix (Figure 2b) included nine scenarios in LS-DYNA (LSTC, Livermore, CA, US), ranging from -90° (forward) to

0° (lateral) and further on to 90° (rearward). The vehicle model was a sedan type provided by our partner (an Original Equipment Manufacturer) and impact severity of the cases was set as 40kph. Component-wise decomposition of knee joint kinematics was then performed to investigate influence of the scenarios. Besides, injury risks of body components were evaluated by cross-sectional moment of tibia and ligament forces.

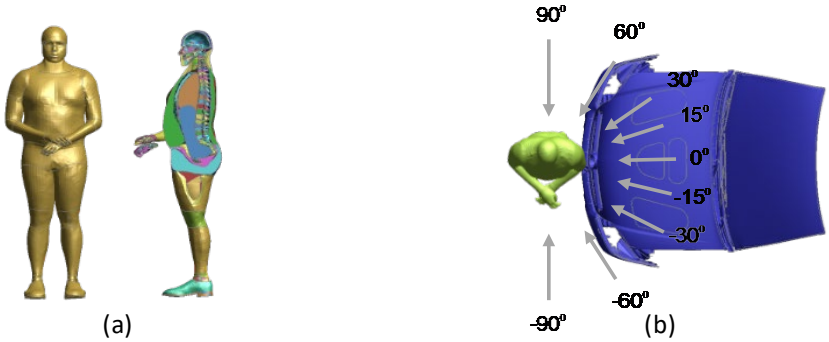

Figure 2. (a) the morphed obese GHBMC pedestrian model (175 cm, BMI 40); (b) setup of simulation matrix and illustration of the sedan model.

III. INITIAL FINDINGS

Peak values of the decomposed kinematics with respect to each DOF are tabulated in Table I. Directions for position values in each DOF are marked with arrows and bolded annotation in Figure 1 (c, d). Patterns of knee joint kinematics are significantly different among scenarios. The maxima of the conventional injurious DOFs – lateral bending and shearing displacement – occur in the pure lateral impact (0°) scenario; and motion in the 15° case was the closest to the planar type because of the smallest magnitude of flexion. The patterns are also asymmetric. Starting from lateral impact, the range of extension brought by forward impact ($0^{\circ} \rightarrow -90^{\circ}$: $-13.08^{\circ} \rightarrow -36.54^{\circ}$) is significantly narrower than the flexion associated with rearward impact ($0^{\circ} \rightarrow 90^{\circ}$: $-13.08^{\circ} \rightarrow 40.14^{\circ}$), indicating flexion is easier to trigger by changing orientation of impact.

TABLE I.
SUMMARY OF PEAK VALUES IN DOFS

Scenarios (Deg.)	Rotational DOFs (Deg.)			Translational DOFs (mm)		
	Flexion	Int. rotation	Abduction	Axial disp.	Shearing disp.	A-P disp.
-90	-36.54	-8.20	-4.27	7.78	3.91	-3.53
-60	-29.96	-4.00	10.96	7.17	4.56	3.42
-30	-22.94	-7.83	17.03	6.42	6.50	4.04
-15	-18.81	-7.58	18.80	5.98	7.95	1.84
0	-13.08	8.92	***23.60***	4.86	***8.92***	1.95
15	***6.01***	12.26	20.86	3.87	6.43	2.85
30	21.06	12.01	14.10	3.32	8.91	3.72
60	36.99	13.03	-8.32	3.07	3.72	4.57
90	40.14	3.81	-7.47	3.10	-3.27	5.32

In terms of injuries, the 15° case is the most dangerous one as it leads to the largest MCL force and tibial moment (Figure 3). Similar with kinematics, asymmetry is also found in injury metrics from pure lateral to fully forward and rearward impacts. Peak values of MCL force and tibial moment are much lower when the impact orientation turns to rearward. In particular, bending moment in tibia is evidently released when the impact orientation changes from 15° to 60°. PCL is loaded on a higher level in forward impacts, while ACL is always loaded on a relatively moderate level (3.5~4.5 kN), regardless of the impact orientation.

IV. DISCUSSION

Computational simulations are cost-effective and time-efficient compared to experimental approaches.

Simulations using human body models remarkably broaden the scenarios of vehicle safety study and offer systematical understanding of human body responses in actual crashes. The current study leveraged highly biofidelic finite element models of the human body to simulate vehicle-to-pedestrian impacts and conducted quantitative analysis of knee joint kinematics and injuries. The main contribution is twofold: 1) established a framework to describe three-dimensional knee joint kinematics; and 2) systematically studied the intrinsic relationship of anatomy, kinematics and injuries to knee joints in vehicle-to-pedestrian impacts.

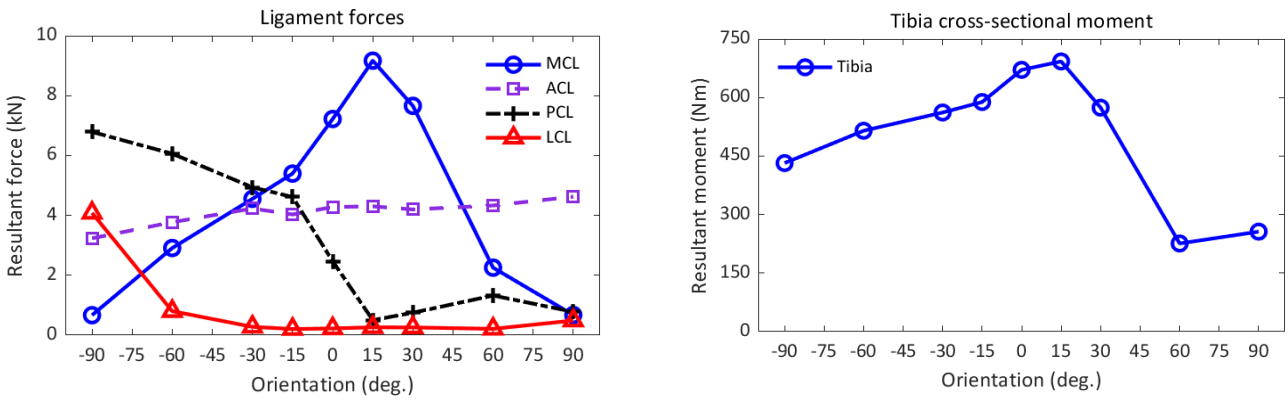

(a) (b)

Figure 3. Variation of injury metrics among scenarios: (a) ligament forces; and (b) tibial cross-sectional moment.

Kinematics bridges the gap between anatomy and injuries at the knee joint. It acts as an effective tool for understanding the discrepancy between patterns of kinematics and tissue-level injuries. As shown in the results, the 15° case corresponding to a maximum MCL force and tibial moment is associated with the smallest out-of-plane flexion (6.01°), while the 0° case with the largest bending angle and shearing displacement is not most dangerous in terms of tissue-level injury metrics. It reflects a fact that conventional injury prediction based on bending and shearing might deliver biased results when applied to three-dimensional scenarios.

Considering the anisotropy of joint anatomy, bending stiffness along flexion is lowest because the natural bending is almost resistance-free. As a consequence, the out-of-plane flexion/extension might potentially unload the system and lead to the inconsistency in terms of kinematical and tissue-level injury predictions. Injury metrics significantly decreases with impact orientation shifted from lateral to rearward (Figure 3b), indicating that flexion is not only easier to trigger but also beneficial to lowering the injury risk. It implies that, if the impact orientation could be adapted towards rearward, it would be helpful for pedestrian safety protection. The idea may guide strategy design for active countermeasures upon an unavoidable collision. For instance, adjusting bumper orientation might result in beneficial effect in protecting the knee joint.

The current work is a pilot study, as a part of a large-scale design of experiments, aiming at investigation on pedestrian lower extremity responses and injuries with respect to various impact scenarios and influential factors. More body sizes and postures (other than the standing obese model here) will be included in future study to better understand the mechanism of how structural anisotropy influences knee joint responses. More experiments and simulations are needed to establish injury criteria of the pedestrian lower-extremity under complicated impact scenarios, and provide reference for test surrogate and countermeasure design. In conclusion, three-dimensional description of knee joint kinematics connects joint anatomy and injuries from impact, and provides reference for countermeasure design from a biomechanical point of view.

V. ACKNOWLEDGEMENTS

This study was supported by National Natural Science Foundation of China (Grant Numbers 51675295, 51975313) and Ministry of Science and Technology of China (Grant Number 2017YFE0118400).

VI. REFERENCES

[1] Kajzer J et al, SAE Transactions, 1997.
[2] Kajzer J et al, SAE Transactions, 1999.
[3] Kerrigan J et al, SAE Technical Paper, 2003.
[4] Grood E et al, J Biomech Eng, 1983.
[5] Tang J et al, IRCOBI conference, 2017.
[6] Tang J et al, Traffic Inj Prev, 2020.